Applied Chemical Engineering (2026) Volume 9 Issue 3 ISSN: 2578-2010 (O)
doi: 10.59429/ace.v9i3.5905

RESEARCH ARTICLE

Synergistic Enhancement of Piezoelectric and Triboelectric Outputs in Barium Titanate/Nylon-11 ($BaTiO_3$/Nylon-11) Nanofibrous Hybrid Nanogenerators for Self-Powered Wearable Electronics

Mokhalad Ali Zbalh[1*], Nawras Hofzi Shliouh[2], Ikram Kamal Jasim[3]

[1] *Applied Biotechnology Department, College of Biotechnology, Al-Qasim Green University, Babylon 51013, Iraq*

[2] *Department of Medical Biotechnology, College of Biotechnology, Al-Qasim Green University, Babylon 51013, Iraq*

[3] *Department of Physics, College of Science, University of Basrah, Basrah-Iraq*

***Corresponding author:** Mokhalad Ali Zbalh, mokhaladali5@gmail.com

ABSTRACT

The growing demand for wearable electronics underscores the need for sustainable, self-sufficient power sources that can effectively convert low-level mechanical energy. This study reports the design and fabrication of a flexible, high-performance hybrid nanogenerator, which utilizes electrospun $BaTiO_3$/Nylon-11 composite nanofibers to harness both piezoelectric and triboelectric effects. Embedding piezoelectric $BaTiO_3$ nanoparticles in a strongly tribopositive Nylon-11 matrix effectively modulates surface charge density through internally generated piezo potential, leading to a significant synergistic increase in triboelectric charge transfer. The optimized hybrid nanogenerator delivers an open-circuit voltage of about 55 V and a short-circuit current of 780 nA, corresponding to a peak power density of 28.4 $\mu W/cm^2$ at an optimal load resistance of 70 M Ω. As a proof of concept for practical applicability, the device instantly powers 30 commercial LEDs under repeated mechanical tapping, demonstrating its strong potential as a self-powered platform for next-generation wearable electronics.

Keywords: Hybrid Nanogenerator, Energy Harvesting, Piezoelectric Effect, Triboelectric Effect, Barium Titanate, Nylon-11, Electrospinning, Wearable Electronics, Synergistic Enhancement.

ARTICLE INFO

Received: 12 February 2026
Accepted: 06 May 2026
Available online: 01 July 2026

1. Introduction

The last decade has witnessed a tremendous boom in the development of wearable electronics, which have become an integral part of diverse fields like personal health monitoring, fitness, and the Internet of Things (IoT). However, the most prominent challenge facing these technologies remains the need for sustainable and independent power sources, conventional batteries suffer from size constraints, limited lifespan, and the need for periodic recharging or replacement, in this context, the concept of harvesting energy from the surrounding environment, particularly from the mechanical movements of the human body, has emerged as an ideal solution for autonomously and continuously powering these device.

Piezoelectric nanogenerators (PENGs) and triboelectric nanogenerators (TENGs) are among the most promising technologies for converting mechanical energy into electrical energy. However, relying on either mechanism alone may limit the overall energy conversion efficiency. For this reason, recent studies have focused on

designing hybrid nanogenerators that combine piezoelectric and triboelectric effects and triboelectricity to achieve synergistic performance enhancement. Studies have shown that this combination is not limited to simply combining the electrical outputs of both mechanisms, but can lead to effective coupling between them, significantly improving device performance.[1] Strategies for enhancing these hybrid generators vary, as advanced techniques such as plasma engineering are employed to modify the materials' microstructure, thereby expanding their response range to different vibrations.[2], the geometric design of the device, like arch-shaped structures[3].

The success of hybrid nanogenerators depends mainly on the careful selection of active materials. Regarding the piezoelectric component, barium titanate ($BaTiO_3$) has received widespread attention for its excellent piezoelectric properties, chemical stability, environmental friendliness, and lead-free status. [4]. To achieve the flexibility required for wearable applications, the material is combined with $BaTiO_3$ nanoparticles within a polymer matrix. A study has shown that controlling the interface between $BaTiO_3$ particles and the surrounding polymer is a crucial factor for enhancing the piezoelectric performance of the final device. [5,6].

To achieve the desired synergistic effect, the host polymer must have dual properties, this is where Nylon-11 comes into play, it not only acts as a flexible and efficient matrix for dispersing $BaTiO_3$ particles, but is also known to be a strongly tribopositive material, making it an Ideal candidate for the active layer in a triboelectric component, the incorporation of $BaTiO_3$ into flexible materials like hydrogel has already demonstrated its potential for use In TENGs and multimodal sensor applications, confirming its ability to work within hybrid systems.[7]. Hence, the fabrication of a $BaTiO_3$/Nylon-11 nanofiber composite by electrospinning offers multiple advantages: it increases the effective surface area for frictional contact, enhances the effective piezoelectric phase (β phase) in the polymer, and provides the device with superior mechanical flexibility. This is consistent with recent trends toward the development of high-performance organic nanogenerators based on nanofiber mats.[8].

Based on the above, this study aims to design and fabricate a flexible hybrid nanogenerator based on barium titanate/nylon-11 ($BaTiO_3$/Nylon-11) nanofiber mats, this study will focus on achieving a synergistic enhancement of the electrical output resulting from both piezoelectric and triboelectric mechanisms by leveraging the dual properties of the materials used and the unique nanostructure, the device's performance in harvesting energy from simple mechanical movements will also be evaluated, paving the way for the development of a new generation of fully autonomous wearable electronics.

2. Literature Review

The development of high-performance hybrid nanogens is based on a deep understanding of the progress made in both active substances and operating mechanisms, in the field of polymeric stresses, study focuses heavily on enhancing the performance of polymers like polyvinylidene fluoride (PVDF), studies have shown that integrating directed nanoscale materials like carbon nanotubes can significantly improve their response to sensing[9], the creation of hybrid compounds like the integration of lead Titans (PZT) zirconies with PVDF has proven effective in energy harvesting applications[10], comprehensive reviews provide a broad view of this area, as developments in pangs are generally summarized[10] with a special focus on promising materials like zinc oxide (ZNO) because of its unique properties in Piezotronics[11,12]. Furthermore, the use of nanowires like nanowires remains an essential strategy to maximize energy conversion efficiency[13,14] to the fundamental physical theories that govern their work[15], to achieve superior performance, various structural and chemical modifications of materials like surface treatment and chemical composition control to increase the density of surface charges generated[16] TENGs has proven its superior energy harvesting from a variety of low-frequency environmental sources, ideal for large-scale applications[17]. A large part of current study is focused on integrating these nano-generators into wearable

electronics to harvest energy from the movement of the human body, the literature reviews the various systems specially designed for this purpose[18] with a special emphasis on wearable TENGS that efficiently transform biomechanical energy[19], this approach extends to the development of the human body IoT integrated IoT systems, where TENGS provide energy and act as sensors at the same time[20], integrating Tengs into textiles also allowed the development of wearable, flexible power sensors[21], innovative designs are directed towards smarter device like TENG generators capable of effectively converting energy harvesting from complex joint movements[22], to achieve full compatibility with the human body, advanced materials like ionic hydrogels are being developed, used in stress sensing.[23]

Parallel to rapid advances in materials science, significant research efforts are currently dedicated to engineering stretchable, self-resilient materials. Also, sweat-resistant wearable devices, where these mechanical properties are crucial for maintaining a stable interface with human skin under dynamic conditions. Enabling the monitoring of vital physiological signals, specifically Electrocardiograms (ECG) and Electromyograms (EMG) - with enhanced precision and superior signal-to-noise ratios[24].

Beyond material fabrication, the study of energy-harvesting physics continues to evolve, focusing on optimizing the fundamental working mechanisms of Triboelectric Nanogenerators (TENGs), including the sophisticated development of Sliding Mode.[25] To maximize surface-area interaction. As well as profound investigations into contact physics and adhesion forces within Vertical Contact-Separation Mode. Understanding these physical interactions is essential for enhancing the electrical output performance and efficiency of generators.[26]

Also, the research trajectory is increasingly directed towards sustainability, emphasizing the use of environmentally friendly, biodegradable materials. Such as cellulose, in the construction of both Piezoelectric Nanogenerators (PENGs) and TENGs[27]. As a result, the application of TENGs in biomedical sensing is gaining substantial momentum, offering promising solutions for continuous health monitoring[28]. To realize the goal of integrated and independent power systems, where direct nanogenerators are now being synergistically coupled with energy storage units, a recent pivotal study demonstrated the capability of PENGs to significantly augment the performance of self-charging supercapacitors (referred to as ultra-factory capacitors). This represents a critical step towards achieving complete self-sufficiency with the provided electronic systems[29]. Final Table 1 presents a comprehensive comparison of the review articles in the provided list, systematically analyzing their specific scope, discussing their research methodologies, and highlighting their key scientific contributions.

Table 1. Comparison of Methodologies in Review Studies

Reference	Focus of the Review	Methodology or Scope of the Study	Key Contribution or Conclusion
[11]	Piezoelectric Nanogenerators (PENGs).	Research review of piezoelectric nanomaterials	Provides an overview of fundamental principles, materials (ZnO, $BaTiO_3$, PVDF), and progress up to 2015.
[12]	ZnO-based Piezotronics and PENGs.	A focused review on ZnO and its applications in PENGs and piezotronics sensors.	Highlights the advantages of ZnO and its potential for a self-powered integrated device.
[13]	ZnO-based Piezoelectric Nanogenerators.	A systematic review covering synthesis methods, characterization techniques, performance enhancement strategies, and applications.	Offers a detailed guide for developing high-performance ZnO-based PENGs.
[15]	Applications of TENG technology.	A broad-scope review of the practical applications of TENGs in diverse fields (sensing, IoT, biomedicine).	Demonstrates the transformative impact of TENG technology and its ability to enable new technologies.

[16]	Theoretical Foundations of TENGs.	A comprehensive theoretical review explaining the physical models and governing equations of TENGs.	Provides the theoretical foundation for understanding, designing, and optimizing TENGs.
[17]	Performance Enhancement of TENGs.	A review focusing on structural and chemical modification strategies to boost electrical output.	Summarizes the methods used to increase surface charge density and improve conversion efficiency.
[19]	Human Motion Energy Harvesting for Wearables.	A comparative review of different harvesting mechanisms (piezoelectric, electromagnetic, triboelectric) and their applications.	Presents a comprehensive analysis of available technologies for powering wearable electronics.
[20]	Wearable TENGs for Biomechanical Energy Harvesting.	A specialized review on the design and materials of TENGs intended for on-body wear.	Focuses on the challenges and solutions related to flexibility, comfort, and efficiency in biomechanical applications.
[22]	Textile-based Force Sensors based on TENGs.	A review focusing on the integration of TENGs into textiles to develop flexible, wearable sensors.	Reviews the latest textile-based electronics.
[28]	Cellulose-based PENGs and TENGs.	A review focusing on the use of sustainable and biocompatible materials (cellulose and its derivatives) for energy harvesting.	Highlights the trend toward green, environmentally friendly electronics.
[29]	TENGs for Biomedical Sensing.	A specialized review on the use of TENGs as active sensors for medical applications.	Illustrates potential TENGs in disease diagnosis and vital sign monitoring.

3. Methodology

3.1. Materials and Chemical Reagents

To ensure the accuracy and reliability of the experimental results, the study relied primarily on a broad, diverse range of precisely defined raw materials and chemical reagents. Each material was obtained from internationally recognized commercial suppliers in the chemical and research industries, which guarantee their compliance with international standards. Since the materials used were of high purity (analytical grade) and met the conditions required for precise reactions, they were also used in the experiments immediately upon receipt. Therefore, these reagents were not subjected to any further purification or pretreatment to avoid potential changes in their chemical composition or physical properties, and to ensure the uniformity at experimental conditions in accordance with principle of scientific integrity and to enable other researchers to follow the investigation and replicate the experiments with the same precision, where the complete identity of each material used was meticulously documented. (2) Table 1 provides a detailed and systematic description of all technical data, including substance names, chemical formulas, and molecular weights (MW/MW). Where purity percentages also depend on particle shape and size.

Table 2. Detailed Specifications of Materials and Chemical Reagents Used

Material Name	Chemical Formula	MW/FW (g/mol)	Purity/Grade	Particle Size/Form	CAS Number	Supplier	Catalog No.
Nylon-11	$[C_{11}H_{21}NO]_n$	~21,000 (Mn)	Polymer Grade	White Pellets	25035-04-5	Arkema, France	Rilsan® BMNO
Barium Titanate	$BaTiO_3$	233.19	99.9% (trace metals basis)	< 100 nm nanopowder (TEM)	12047-27-7	Sigma-Aldrich, USA	631662

Formic Acid	HCOOH	46.03	≥ 98% (ACS reagent)	Clear Liquid	64-18-6	Sigma-Aldrich, USA	F0507
Dimethylformamide (DMF)	C_3H_7NO	73.09	≥ 99.8% (Anhydrous)	Clear Liquid	68-12-2	Merck, Germany	1.03054
Copper Tape	Cu	63.55	99.9%	Conductive adhesive tape, 50 µm thickness	7440-50-8	3M, USA	1181
Polydimethylsiloxane (PDMS)	$[SiO(CH_3)_2]_n$	-	SYLGARD™ 184 Kit	Viscous Liquid (Base & Curing Agent)	63148-62-9	Dow Corning, USA	184

3.2. Preparation of the $BaTiO_3$/Nylon-11 Composite Electrospinning Solution

The preparation of electroforming solutions is a crucial step for the quality of the resulting fibers. Therefore, special attention was paid to the preparation of both pure and composite polymer solutions to precisely adjust their rheological properties, particularly viscosity and electrical conductivity, to meet the requirements of the electroforming process. The process began with the preparation of a base solution by dissolving 15% (w/v) nylon-11 granules in a binary solvent system of formic acid and dimethylformamide (DMF) in an 80:20 volumetric ratio. The mixture composition provided an optimal balance between polymer solubility and solvent evaporation rate. To ensure complete homogeneity and total decomposition of the polymer chains, the mixture was stirred for 12 hours at 40 ° C and 500 rpm using a magnetic stirrer.

In parallel, suspensions of barium titanate ($BaTiO_3$) nanoparticles at different concentrations in DMF were prepared due to the nanoparticles' natural tendency to agglomerate. These suspensions were dispersed for 30 minutes using a 100 W ultrasonic probe. This critical step was performed in an ice bath to control the heat generated by the ultrasonic waves and prevent the solution from overheating. This ensured particle separation and prevented deagglomeration. Once dispersion was complete, the homogenized barium titanate suspension was slowly and carefully added to the previously prepared nylon-11 solution. Subsequently, a final mixing process was initiated, lasting 6 hours with constant magnetic stirring. The composition of the resulting solution and its physical properties are presented in Table 3.

Table 3. Compositions and Properties of the Prepared Electrospinning Solutions

Sample ID	Mass of Nylon-11 (g)	Mass of $BaTiO_3$ (g)	Volume of Formic Acid (mL)	Volume of DMF (mL)	Weight ratio of $BaTiO_3$ to polymer (wt%)	Total Solute Concentration (w/v %)	Measured Viscosity @25°C (cP)
BN-0	1.5	0.00	8	2	0%	15.0	~1250
BN-5	1.5	0.075	8	2	5%	15.75	~1310
BN-10	1.5	0.150	8	2	10%	16.5	~1380
BN-15	1.5	0.225	8	2	15%	17.25	~1460
BN-20	1.5	0.300	8	2	20%	18.0	~1550

3.3. Fabrication of Nanofiber Mats via Electrospinning

An advanced electrospinning setup (NS-LAB, Elmarco) was utilized to convert the prepared solutions into non-woven nanofiber mats. All the solutions were taken and placed in a plastic syringe. This syringe had a capacity of 10 ml and a 21 mm metal needle (0.51 mm internal diameter). All process parameters were precisely controlled and recorded, as detailed in Table 4, to ensure consistent and comparable fiber morphology across different samples. The nanofibers were collected on an aluminum foil-covered rotating drum for 4 hours per sample to produce mats with an approximate thickness of 100 µm.

Table 4. Fixed, Controlled Parameters Electrospinning Process

Parameter	Set Value	Unit	Notes / Purpose
Applied Voltage	18	kV	To achieve a stable Taylor cone and stretching of the polymer jet
Solution Flow Rate	0.8	mL/h	To ensure an appropriate solvent evaporation rate before fiber deposition
Tip-to-Collector Distance	15	cm	To balance the time of flight and the electric field strength
Needle Inner Diameter	0.51 (21 Gauge)	mm	To control the initial droplet size and flow stability
Collector Type	Rotating Drum	-	To obtain randomly oriented fibers and a uniform mat thickness
Collector Rotation Speed	200	rpm	To aid in the even distribution of fibers
Spinning Duration per Sample	4	hours	To achieve a target mat thickness of ~100 μm
Ambient Temperature	25 ± 2	°C	To maintain constant solution viscosity and evaporation rate
Relative Humidity	45 ± 5	%	To prevent needle clogging and its influence on surface properties
Post-Spinning Treatment	Vacuum drying at 60°C for 24 h	-	To completely remove residual solvents.

3.4. Assembly of the Hybrid Nanogenerator Device

The flexible hybrid device was assembled following a meticulous protocol to ensure good electrical contact and proper insulation. The process began with the preparation of a 3 cm × 3 cm, 1 mm-thick flexible PDMS substrate. A conductive copper tape (2 cm × 2 cm) was adhered to the substrate surface as the bottom electrode, then the optimized composite nanofiber mat ($BaTiO_3$/Nylon-11),

Finally, the entire device was encapsulated with a PDMS mixture (10:1 base-to-curing agent ratio), leaving the top electrode exposed for mechanical contact, and the encapsulation was thermally cured at 70° C for 2 hours.

3.5. Materials and Device Characterization

An extensive range of tests was performed to determine the morphological, structural, compositional, thermal, and mechanical properties of the fabricated nanofibers. Table 5 details the characterization techniques, instruments used, and key parameters for every analysis.

Table 5. Techniques and Instruments Used for Material and Device Characterization

Technique	Purpose of Analysis	Instrument Model & Manufacturer	Key Analysis Parameters & Conditions
Scanning Electron Microscopy (SEM)	To analyze fiber morphology, measure average fiber diameters, and examine surface particle distribution.	JEOL JSM-7600F FE-SEM	Acceleration Voltage: 5-10 kV, working Distance: 8-10 mm, detector: SEI, sample Coating: 5 nm Au/Pd, image analysis via ImageJ software.
Transmission Electron Microscopy (TEM)	To set the presence and dispersion of $BaTiO_3$ nanoparticles within the nanofibers and determine their crystalline structure.	FEI Tecnai G2 F20 S-TWIN	Acceleration Voltage: 200 kV; samples were prepared by directly electrospinning fibers onto carbon-coated copper grids for ease of preparation.
FTIR-ATR Spectroscopy	To identify functional groups, confirm the piezoelectric β-phase in Nylon-11, and monitor molecular interactions.	Thermo Fisher Nicolet iS50	Mode: ATR with a diamond crystal.
Differential Scanning Calorimetry (DSC)	To study thermal behavior, determine melting and crystallization temperatures, and calculate the degree of crystallinity.	TA Instruments Q200	Temperature Range: 20-250°C.
Mechanical Testing	Evaluate mechanical properties at mats (Young's modulus, tensile strength, elongation at break).	Instron 5967 Universal Testing Machine	Strain Rate: 10 mm/min; sample dimensions according to ASTM D882. An average of 5 specimens per composition was tested.

3.6. Electrical Performance Measurement

The electrical performance of the hybrid nanogenerator was evaluated under precisely controlled mechanical conditions to simulate practical applications. A linear motor (LinMot E1100) connected to a precision controller was used to apply a periodic compressive force to the device's effective area. Experiments were designed to isolate and understand the contribution of each mechanism (piezoelectric and triboelectric) to the total output and to determine the optimal power output. The device was connected to a circuit with variable load resistances, and the power was calculated for each resistance. The testing parameters are summarized in Table 6.

Table 6. Parameters and Conditions for Electrical Performance Testing

Parameter	Range / Value	Unit	Instrument / System Used
Applied Force	0.5 - 10	N (Newton)	LinMot E1100 Linear Motor with Force Sensor
Force Frequency	1 - 10	Hz	LinMot Controller
Force Waveform	Square Wave	-	Programmed to simulate rapid contact and separation
Effective Contact Area	4 (2x2)	cm^2	-
Load Resistance	10^3 - 10^9	Ω (Ohm)	Decade Resistance Box
Data Acquisition System	Keithley 6517B Electrometer / NI-DAQ	-	Interfaced with LabVIEW for data logging
Voltage Measurement	Voc (Open-circuit Voltage)	V	Keithley 6517B (Input Impedance > 200 TΩ)
Current Measurement	Isc (Short-circuit Current)	nA / µA	Keithley 6517B (in Ammeter mode)

4. Results

4.1. Morphological and Structural Characterization of Nanofibers

Fig1(a) shows the morphology at nanofibers of the pure sample (BN-0), the fibers appear regular and have smooth surfaces, indicating the successful electrospinning of the pure Nylon-11 solution, in contrast, the images of the optimized sample (BN-15) in Figure 1(b) show fibers with slight surface roughness, which is attributed to the presence of $BaTiO_3$ nanoparticles embedded near the fiber surface, (TEM) examination in Fig1(c) confirms the homogeneous distribution $BaTiO_3$ particles (visible as dark dots) within the Nylon-11 fiber matrix (light gray background) without the presence of large agglomerates.

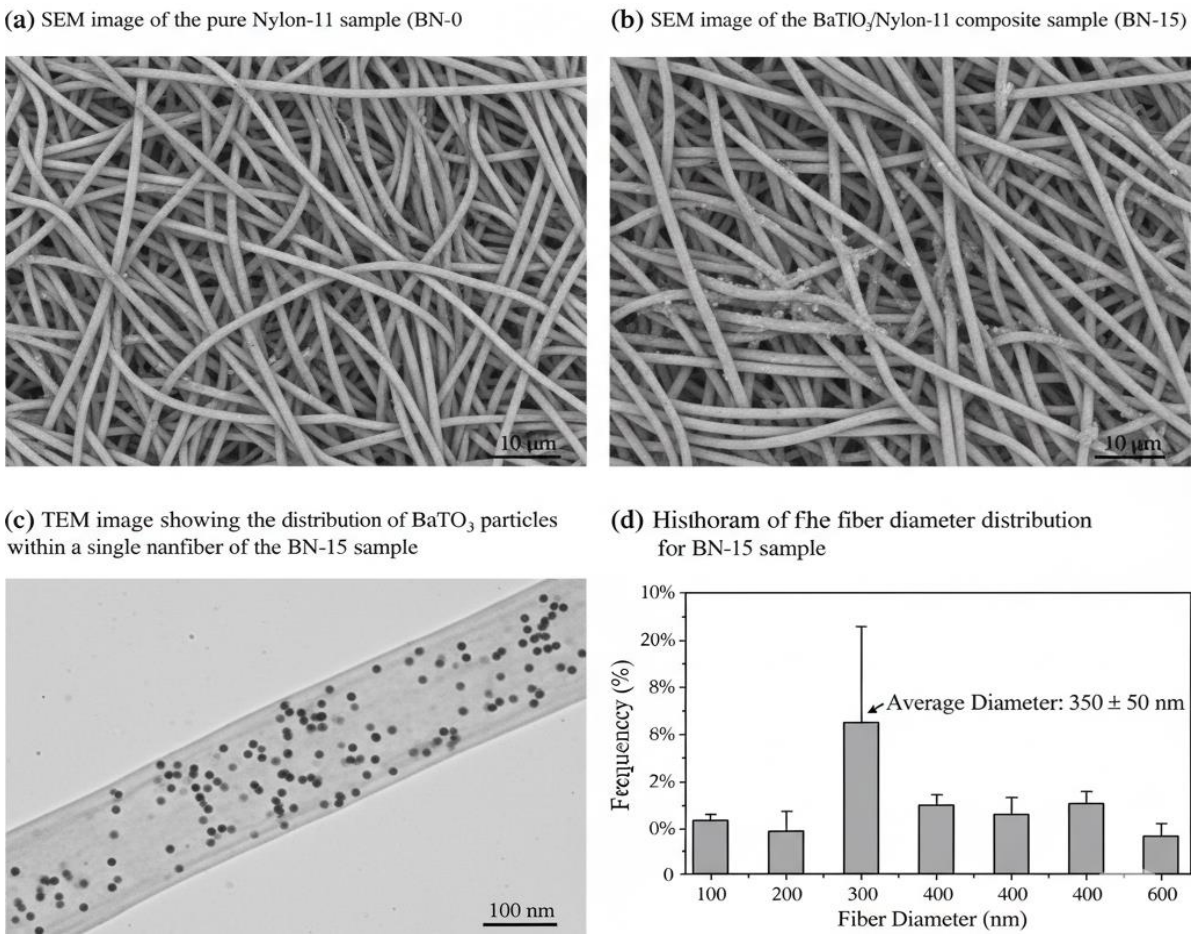

Figure 1. Morphological analysis of nanofiber mats. (a) SEM image of the pure Nylon-11 sample (BN-0). (b) SEM image of the $BaTiO_3$/Nylon-11 composite sample (BN-15). (c) TEM image showing the distribution of $BaTiO_3$ particles within a single nanofiber of the BN-15 sample. (d) Histogram of the fiber diameter distribution for the BN-15 sample.

Figure 2 shows the characteristic crystalline peaks of the perovskite $BaTiO_3$ phase in all synthesized samples, confirming the successful integration of the perovskite phase. For pure Nylon-11 (BN-0), a broad peak appears at $2\theta \approx 21.5^\circ$, representing a superposition of the non-piezoelectric α and γ phases, interestingly, in the BN-15 sample, this peak becomes sharper, and minor additional peaks appear, indicating an increased degree of crystallinity and enhanced formation of the piezoelectric β-phase, this conclusion is conclusively confirmed by the FTIR spectra in Figure 2(b), where the characteristic absorption bands of the beta phase at 840 cm^{-1} and 1275 cm^{-1} are more pronounced in the BN-15 sample than in the pure sample, demonstrating that the presence of $BaTiO_3$ particles under the influence of a high electric field during spinning enhances the molecular orientation required for piezoelectric activity.

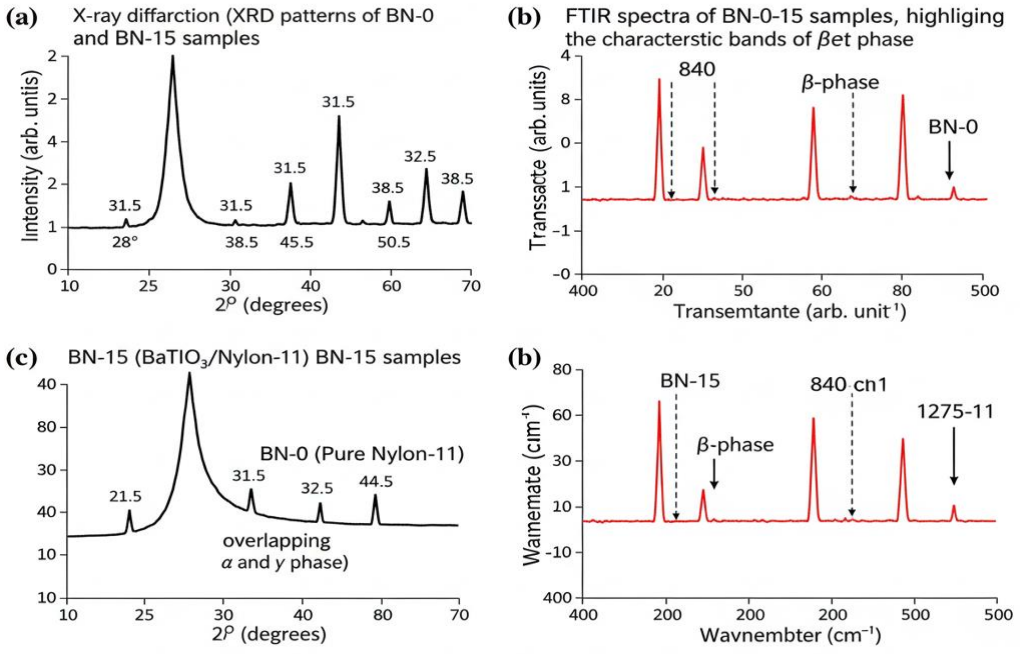

Figure 2. Compositional and structural analysis

4.2. Hybrid Nanogen Performance and Synergistic Effect

The main contribution of this work is to demonstrate synergistic enhancement resulting from the coupling of piezoelectric and triboelectric effects—Figure 3. A direct comparison of electrical output is shown in the "piezoelectric-only mode," where the device was isolated from any external friction. The BN-15 sample produced modest amounts. ($V_{oc} \approx 3.5\,V, I_{sc} \approx 60\,nA$) Due to the pressure-induced polarization of $BaTiO_3$ and Nylon-11 (β-phase) in the "triboelectric-only mode," the pure Nylon-11 (BN-0) sample generated a much higher output. ($V_{oc} \approx 22\,V, I_{sc} \approx 250\,nA$) When rubbed against a copper surface, in hybrid mode, the BN-15 demonstrated remarkably superior performance, reaching an output of ($V_{oc} \approx 55\,V, I_{sc} \approx 780\,nA$), Far exceeding the arithmetic sum of the two individual outputs, this synergistic enhancement is attributed to the internally generated piezoelectric potential, which modulates the surface potential barrier, significantly increasing the density of triboelectric charges transferred during contact and separation cycles. Figure 4 shows typical voltage and current waveforms for the hybrid device, with positive and negative peaks corresponding to compression and release movements, respectively.

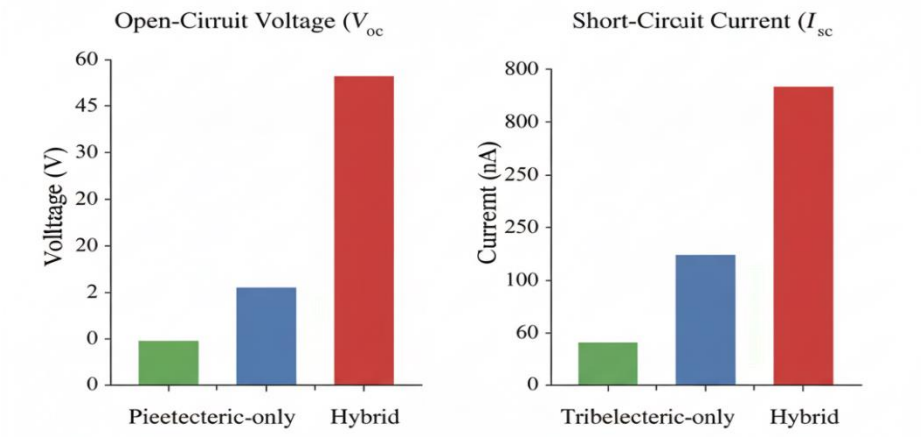

Figure 3. Demonstration of the synergistic effect.

(a) Open-circuit voltage waveform

(b) Short-circuit current waveform under a cyclic force of 5 N

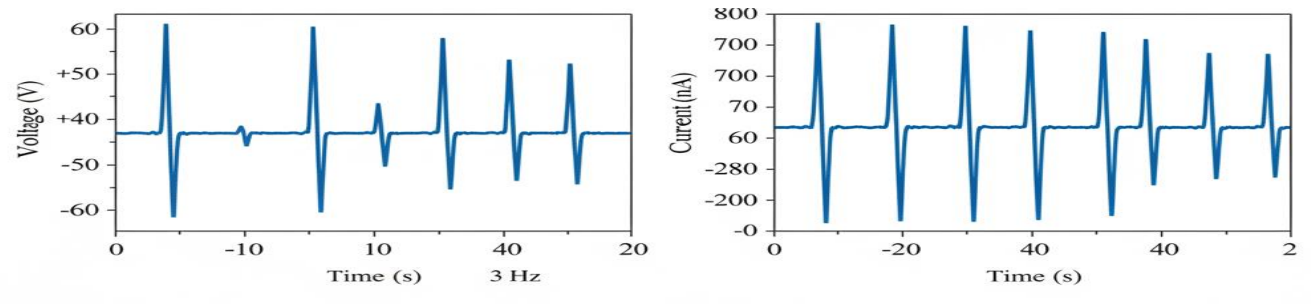

Figure 4. Typical electrical output hybrid device (BN-15).

4.3. Performance Optimization and Variables Study

Increasing $BaTiO_3$ content, reaching a maximum at 15 wt% (BN-15), and then decreasing at 20 wt%, is attributed to the fact that, up to 15 wt%, $BaTiO_3$ particles increase the dielectric constant and enhance piezoelectric polarization. However, at higher concentrations, particle agglomeration may lead to increased charge leakage and reduced mechanical flexibility, impairing overall performance. The response of the optimized device (BN-15) to varying applied mechanical force and frequency was also evaluated (Figure 6). Figure 6(a) shows that the electrical output increases almost linearly with increasing force from 1 to 10 N, due to increased mechanical deformation and the effective contact area. Similarly, Figure 6(b) shows an increase in output with increasing frequency from 1 to 10 Hz, where a faster rate of contact and separation results in a greater flow of charge per unit time.

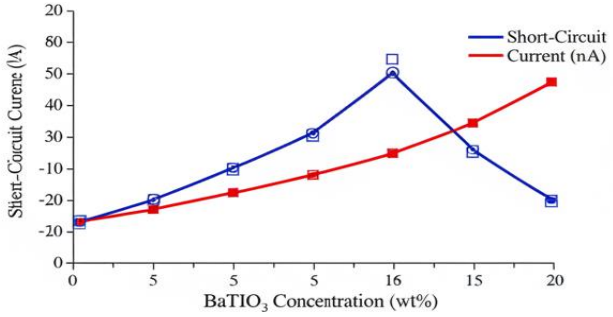

Figure 5. Effect of $BaTiO_3$ concentration on the electrical output of the hybrid device

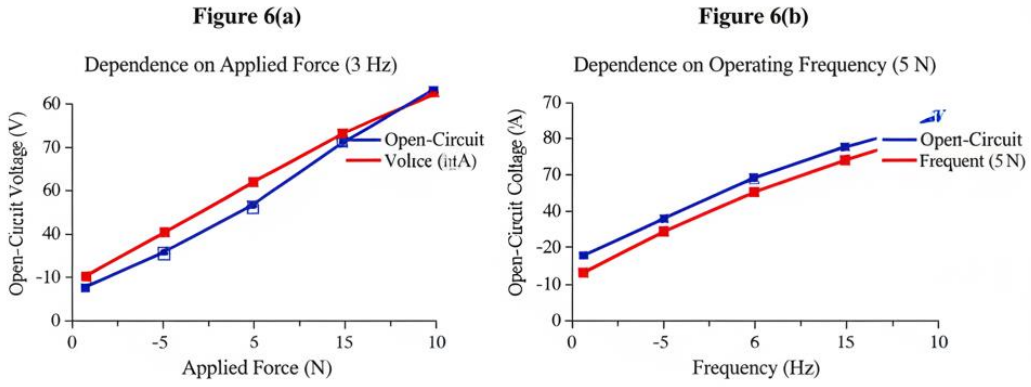

Figure 6. Effect of mechanical variables on the performance of the BN-15 device.

5. Discussion

The obtained results clearly demonstrate that the hybrid approach adopted in this work, which combines both piezoelectric and triboelectric effects within a single nanofiber structure, results in a significant synergistic enhancement in energy harvesting performance, but far exceeds them, this synergistic enhancement can be explained by the piezo-triboelectric coupling mechanism, when compressive force is applied, the $BaTiO_3$ particles and the beta phase of Nylon-11 not only generate a piezoelectric potential, but this generated internal potential also modifies the surface potential of the nanofiber mat, the piezoelectric effect acts as an internal "amplifier" for the triboelectric effect, a phenomenon consistent with recent observations in other hybrid systems.[1] and confirming the validity of theoretical models linking TENG performance to the surface potential of materials[15].

The success of this synergistic effect is primarily due to the thoughtful design of the material and structure. Nylon-11 was chosen not only for its flexibility and electrospinning ability, but also because it is a material with strong cation city, creating a significant triboelectric potential difference with copper, importantly, the electrospinning process under a high electric field, with $BaTiO_3$ nanoparticles as confirmed by XRD and FTIR results, this is consistent with studies aimed at developing high-performance organic nanogenerators based on nanofiber mats[8].

The ability to easily light up 30 LEDs with a simple mechanical tap confirms the device's practical feasibility. This level of power output is sufficient to power numerous low-power sensors or transmit data intermittently in human body IoT systems.[20] This work opens the door to the development of a new generation of smart textiles and biomedical devices.[28] Those that do not require external batteries, however, there is still room for future improvements. A future study could focus on directly integrating the device with energy storage units, such as flexible supercapacitors, to create a fully integrated, autonomous power system, similar to what has been proposed in other studies linking generators and storage units.[29-31] The effect of chemical surface modification of the fibers to increase charge density could also be investigated, and the possibility of fabricating the device on real textile substrates to achieve superior wearability and comfort could be explored.

6. Conclusion

This study successfully operated a flexible hybrid nanogenerator based on nanofibers composed of $BaTiO_3$ and nylon-11. The key result is a significant synergistic improvement in electrical performance. This remarkable improvement is due to the dynamic interaction between the piezoelectric potential generated by the $BaTiO_3$ molecules and the β phase of nylon-11 molecules, combined with the piezoelectric effect at the generator's contact surface.

Furthermore, the advantages of this innovation extend beyond superior electrical performance and include mechanical strength, structural flexibility, and the use of environmentally friendly materials. These exceptional properties make this hybrid generator a promising and reliable candidate for powering a wide range of low-power wearable electronic devices, from health monitoring sensors to human-machine interfaces.

These results open new horizons for the development of more advanced autonomous energy systems and lay methodological groundwork for integrating this technology into smart textiles and for creating integrated autonomous modules for each energy generation and storage process. Considering these promising results, the study recommends exploring the potential for improved performance through better material texture and structure, as well as more precise electrode geometry design. As well as exploring mechanisms for integrating these advanced generators into functional bright textures and IOT systems to create self-sufficient, integrated, and efficient energy systems.

References

1. D. Sarkar, N. Das, M.M. Saikh, S. Roy, S. Paul, N.A. Hoque, R., Basu, S., Das, Elevating the performance of nanoporous bismuth selenide incorporated arch-shaped triboelectric nanogenerator by implementing piezo-tribo coupling effect: harvesting biomechanical energy and low-scale energy sensing applications, Advanced Composites and Hybrid Materials 6 (2023) 232. https://doi.org/10.1007/s42114-023-00807-0.
2. X. García-Casas, A. Ghaffarinejad, F.J. Aparicio, J. Castillo-Seoane, C. López-Santos, J.P. Espinós, J. Cotrino, J.R. Sánchez-Valencia, Á. Barranco, A. Borrás, Plasma engineering of microstructured piezo – Triboelectric hybrid nanogenerators for wide bandwidth vibration energy harvesting, Nano Energy 91 (2022) 106673. https://doi.org/10.1016/j.nanoen.2021.106673.
3. C. Xue, J. Li, Q. Zhang, Z. Zhang, Z. Hai, L. Gao, R. Feng, J. Tang, J. Liu, W. Zhang, D. Sun, A Novel Arch-Shape Nanogenerator Based on Piezoelectric and Triboelectric Mechanism for Mechanical Energy Harvesting, Nanomaterials 5 (2014) 36 – 46. https://doi.org/10.3390/nano5010036.
4. O. Okhay, A. Tkach, Current Achievements in Flexible Piezoelectric Nanogenerators Based on Barium Titanate, Nanomaterials 13 (2023) 988. https://doi.org/10.3390/nano13060988.
5. K. Shi, B. Chai, H. Zou, P. Shen, B. Sun, P. Jiang, Z. Shi, X. Huang, Interface-induced performance enhancement in flexible BaTiO3/PVDF-TrFE-based piezoelectric nanogenerators, Nano Energy 80 (2021) 105515. https://doi.org/10.1016/j.nanoen.2020.105515.
6. S.-H. Shin, S.-Y. Choi, M.H. Lee, J. Nah, High-Performance Piezoelectric Nanogenerators via Imprinted Sol – Gel BaTiO 3 Nanopillar Array, ACS Applied Materials & Interfaces 9 (2017) 41099 – 41103. https://doi.org/10.1021/acsami.7b11773.
7. Z. Wang, Z. Liu, G. Zhao, Z. Zhang, X. Zhao, X. Wan, Y. Zhang, Z.L. Wang, L. Li, Stretchable Unsymmetrical Piezoelectric BaTiO 3 Composite Hydrogel for Triboelectric Nanogenerators and Multimodal Sensors, ACS Nano 16 (2022) 1661 – 1670. https://doi.org/10.1021/acsnano.1c10678.
8. K. Maity, D. Mandal, All-Organic High-Performance Piezoelectric Nanogenerator with Multilayer Assembled Electrospun Nanofiber Mats for Self-Powered Multifunctional Sensors, ACS Applied Materials & Interfaces 10 (2018) 18257 – 18269. https://doi.org/10.1021/acsami.8b01862.
9. S. Sharafkhani, M. Kokabi, Enhanced sensing performance of polyvinylidene fluoride nanofibers containing preferred oriented carbon nanotubes, Advanced Composites and Hybrid Materials 5 (2022) 3081 – 3093. https://doi.org/10.1007/s42114-022-00565-5.
10. S.H. Wankhade, S. Tiwari, A. Gaur, P. Maiti, PVDF – PZT nanohybrid based nanogenerator for energy harvesting applications, Energy Reports 6 (2020) 358 – 364. https://doi.org/10.1016/j.egyr.2020.02.003.
11. R.K. Pandey, J. Dutta, S. Brahma, B. Rao, C.-P. Liu, Review on ZnO-based piezotronics and piezoelectric nanogenerators: aspects of piezopotential and screening effect, Journal of Physics: Materials 4 (2021) 044011. https://doi.org/10.1088/2515-7639/ac130a.
12. A.T. Le, M. Ahmadipour, S.-Y. Pung, A review on ZnO-based piezoelectric nanogenerators: Synthesis, characterization techniques, performance enhancement and applications, Journal of Alloys and Compounds 844 (2020) 156172. https://doi.org/10.1016/j.jallcom.2020.156172.
13. Z. Wang, X. Pan, Y. He, Y. Hu, H. Gu, Y. Wang, Piezoelectric Nanowires in Energy Harvesting Applications, Advances in Materials Science and Engineering 2015 (2015) 1 – 21. https://doi.org/10.1155/2015/165631.
14. D. Jiang, M. Lian, M. Xu, Q. Sun, B. Bin Xu, H.K. Thabet, S.M. El-Bahy, M.M. Ibrahim, M. Huang, Z. Guo, Advances in triboelectric nanogenerator technology—applications in self-powered sensors, Internet of Things, biomedicine, and blue energy, Advanced Composites and Hybrid Materials 6 (2023) 57. https://doi.org/10.1007/s42114-023-00632-5.
15. H. Zhang, L. Yao, L. Quan, X. Zheng, Theories for triboelectric nanogenerators: A comprehensive review, Nanotechnology Reviews 9 (2020) 610 – 625. https://doi.org/10.1515/ntrev-2020-0049.
16. Y. Nurmakanov, G. Kalimuldina, G. Nauryzbayev, D. Adair, Z. Bakenov, Structural and Chemical Modifications Towards High-Performance of Triboelectric Nanogenerators, Nanoscale Research Letters 16 (2021) 122. https://doi.org/10.1186/s11671-021-03578-z.
17. J. Tian, X. Chen, Z.L. Wang, Environmental energy harvesting based on triboelectric nanogenerators, Nanotechnology 31 (2020) 242001. https://doi.org/10.1088/1361-6528/ab793e.
18. M. Cai, Z. Yang, J. Cao, W.-H. Liao, Recent Advances in Human Motion Excited Energy Harvesting Systems for Wearables, Energy Technology 8 (2020). https://doi.org/10.1002/ente.202000533.
19. Y. Zou, V. Raveendran, J. Chen, Wearable triboelectric nanogenerators for biomechanical energy harvesting, Nano Energy 77 (2020) 105303. https://doi.org/10.1016/j.nanoen.2020.105303.

20. Q. Zhang, C. Xin, F. Shen, Y. Gong, Y. Zi, H. Guo, Z. Li, Y. Peng, Q. Zhang, Z.L. Wang, Human body IoT systems based on the triboelectrification effect: energy harvesting, sensing, interfacing and communication, Energy & Environmental Science 15 (2022) 3688 – 3721. https://doi.org/10.1039/D2EE01590K.
21. C. Hu, F. Wang, X. Cui, Y. Zhu, Recent progress in textile-based triboelectric force sensors for wearable electronics, Advanced Composites and Hybrid Materials 6 (2023) 70. https://doi.org/10.1007/s42114-023-00650-3.
22. S. Cho, Y. Yun, S. Jang, Y. Ra, J.H. Choi, H.J. Hwang, D. Choi, D. Choi, Universal biomechanical energy harvesting from joint movements using a direction-switchable triboelectric nanogenerator, Nano Energy 71 (2020) 104584. https://doi.org/10.1016/j.nanoen.2020.104584.
23. T. Li, H. Wei, Y. Zhang, T. Wan, D. Cui, S. Zhao, T. Zhang, Y. Ji, H. Algadi, Z. Guo, L. Chu, B. Cheng, Sodium alginate reinforced polyacrylamide/xanthan gum double network ionic hydrogels for stress sensing and self-powered wearable device applications, Carbohydrate Polymers 309 (2023) 120678. https://doi.org/10.1016/j.carbpol.2023.120678.
24. J.-W. Li, B.-S. Huang, C.-H. Chang, C.-W. Chiu, Advanced electrospun AgNPs/rGO/PEDOT: PSS/TPU nanofiber electrodes: Stretchable, self-healing, and perspiration-resistant wearable devices for enhanced ECG and EMG monitoring, Advanced Composites and Hybrid Materials 6 (2023) 231. https://doi.org/10.1007/s42114-023-00812-3.
25. W.-Z. Song, H.-J. Qiu, J. Zhang, M. Yu, S. Ramakrishna, Z.L. Wang, Y.-Z. Long, Sliding mode direct current triboelectric nanogenerators, Nano Energy 90 (2021) 106531. https://doi.org/10.1016/j.nanoen.2021.106531.
26. W. Yang, X. Wang, P. Chen, Y. Hu, L. Li, Z. Sun, On the controlled adhesive contact and electrical performance of vertical contact-separation mode triboelectric nanogenerators with micro-grooved surfaces, Nano Energy 85 (2021) 106037. https://doi.org/10.1016/j.nanoen.2021.106037.
27. Y. Song, Z. Shi, G.-H. Hu, C. Xiong, A. Isogai, Q. Yang, Recent advances in cellulose-based piezoelectric and triboelectric nanogenerators for energy harvesting: a review, Journal of Materials Chemistry A 9 (2021) 1910 – 1937. https://doi.org/10.1039/D0TA08642H.
28. T. Tat, A. Libanori, C. Au, A. Yau, J. Chen, Advances in triboelectric nanogenerators for biomedical sensing, Biosensors and Bioelectronics 171 (2021) 112714. https://doi.org/10.1016/j.bios.2020.112714.
29. D. Zhou, N. Wang, T. Yang, L. Wang, X. Cao, Z.L. Wang, A piezoelectric nanogenerator promotes highly stretchable and self-chargeable supercapacitors, Materials Horizons 7 (2020) 2158 – 2167. https://doi.org/10.1039/D0MH00610F.
30. Li W, Song Z, He Y, Zhang J, Bao Y, Wang W, Sun Z, Ma Y, Liu Z and Niu L (2023) Natural sedimentation-assisted fabrication of Janus functional films for versatile applications in Joule heating, electromagnetic interference shielding and triboelectric nanogenerator. Chem Eng J 455:140606. doi: https://doi.org/10.1016/j.cej.2022.140606.
31. Song Z, Li W, Kong H, Bao Y, Wang N, Wang W, Ma Y, He Y, Gan S and Niu L (2022) Enhanced energy harvesting performance of triboelectric nanogenerator via efficient dielectric modulation dominated by interfacial interaction. Nano Energy 92:106759. doi: https://doi.org/10.1016/j.nanoen.2021.106759.